

Lihui WANG, Dayu LIU, Bo WANG, Jie SUN, Lianhong LI

Design of parallel microfluidic gradient-generating networks for studying cellular response to chemical stimuli

© Higher Education Press and Springer-Verlag 2008

Abstract A microfluidic chip featuring laminar flow-based parallel gradient-generating networks was designed and fabricated. The microchip contains 5 gradient generators and 30 cell chambers where the resulting concentration gradients of drugs are delivered to stimulate on-chip cultured cells. The microfluidics exploits the advantage of lab-on-a-chip technology by integrating the generation of drug concentration gradients and a series of cell operations including seeding, culture, stimulation and staining into a chip. The microfluidic network was patterned on a glass wafer, which was further bonded to a PDMS film. A series of weir structures were fabricated on the cell culture reservoir to facilitate cell positioning and seeding. Cell injection and fluid delivery were controlled by a syringe pump. Steady parallel concentration gradients were generated by flowing two fluids in each network. Over time observation shows that the microchip was suitable for cell seeding and culture. The microchip described above was applied in studying the role of reduced glutathione (GSH) in mediating chemotherapy sensitivity of MCF-7 cells. MCF-7 cells were treated with concentration gradients of As_2O_3 and N-acetyl cysteine (NAC) for GSH modulation, followed by exposure to adriamycin. GSH levels were down-regulated upon As_2O_3 treatment and up-regulated upon NAC treatment. Suppression of intracellular GSH by treatment with As_2O_3 has been shown to increase sensitivity to adriamycin. Conversely, elevation of intracellular GSH by treatment with NAC leads to increased drug resistance. The integrated microfluidic chip is able to perform multiparametric pharmacological profiling with

easy operation, and thus holds great potential for extrapolation to the cell based high-content drug screening.

Keywords microfluidic chip, gradient concentration, laminar flow, cell

1 Introduction

Multiple chemical stimuli such as hormones, metabolites and drugs mediate cellular activity *in vivo*. Investigation of the interplay between the intensity of chemical stimulations and corresponding cellular response may be helpful to find the mechanisms regulating specific cellular activities and develop controlled microenvironments to produce desired cellular response. Since the common paradigm in cell biology is the dose-dependent interaction of mediators in determining cellular responses, the study of cellular response typically includes exposing cells to a gradient concentration of chemical stimulation and observing the cellular response over time. As those studies with conventional methods are usually labor intensive and consumes reagents, systems that integrate those steps would greatly simplify the operation.

Microfluidic technology is conceptually well suited for the development of flexible and integrated *in vitro* systems allowing high-throughput analysis of cells under large numbers of conditions [1–3]. The Microfluidic chip has many advantages over conventional systems, such as the perfusion fluidic behavior and comparable size to the capillary system that is suitable for cell culture with the environments similar to that *in vivo*, integration of steps for cell research to simplify the operation and realization of high-throughput expression of cellular activity. In recent studies, laminar flow-based linear gradient generation has been demonstrated as a feature of microfluidic devices for studying cellular response to chemical stimulation [1]. With these devices, it is possible to treat a cell population with a controlled chemical gradient and observe biochemical and morphological responses *in vitro*. The continuously flowing streams of fluid provide

Translated from *Chinese Journal of Analytical Chemistry*, 2008, 36(2): 143–149

Lihui WANG, Bo WANG, Jie SUN, Lianhong LI (✉)
Department of Pathology, Dalian Medical University, Dalian 116044, China
E-mail: ruark@126.com

Dayu LIU
Dalian Institute of Chemical Physics, Chinese Academy of Sciences,
Dalian 116023, China
Biomedical Engineering Center, Improve Medical Instrument's Co.,
Ltd., Guangzhou 510370, China

precise control over the stability, gradient profile, concentration range and slope of a chemical gradient.

Microfluidic channel has diameter ranging from tens to hundreds of micrometers, in which liquids that flow slowly follow predictable laminar paths characteristic of low Reynolds numbers [4]. This character allows two or more layers of fluid to flow next to each other without any mixing other than by diffusion of their constituent molecular and particulate components. By flowing two or more fluids of flow each carrying different concentrations of substances through microfluidic networks of appropriately designed layout, complex gradients can generate through controlled diffusive mixing of substances [5,6]. The flexibility of microfluidic chip enables design and fabrication of complex microfluidic networks, thus providing a way to simulate complex heterogeneities in concentrations *in vivo* [7–9].

In this study, a microfluidic chip featuring parallel gradient-generating networks was designed and fabricated. This microfluidics integrated the generation of drug concentration gradients and a series of cell operations including seeding, culture, stimulation and staining into a chip. Such a microchip was investigated for generation of parallel gradients and was applied for generating gradients of modulators to stimulate breast cancer MCF-7 cells for studying the role of GSH in mediating chemotherapy sensitivity of MCF-7 cells. The microfluidic chip-based cellular response assay exploits advantages of lab-on-a-chip technology, flexibility, integration and high throughput.

2 Experimental

2.1 Instrument and reagents

Glass plate with positive photoresist (Shaoguang, Changsha, Hunan, China) and PDMS film of 300 μm thickness (HT6240, Rogers Corp., USA) were used for the fabrication of the microfluidic chip. A syringe pump (Kloehn, USA) and fluorescent microscope (BX41, Olympus Inc., Tokyo, Japan) were used. The arsenic trioxide (As_2O_3), fluorescein sodium and N-acetyl cysteine (NAC) were purchased from Sigma (St. Louis, Mo, USA). Naphthalene-2, 3-dicarboxaldehyde (NDA) was purchased from Molecular Probes (Eugene, OR, USA). Acridine orange (AO) and ethidium bromide (EB) was purchased from Amresco (Solon, Ohio, USA). Adriamycin was purchased from Pharmacia-Upjohn (Milan, Italy). Working solutions of fluorescent dye were prepared with PBS solution. The concentration of NDA working solution was 5×10^{-6} mol/L, while that of AO and EB was 2.5 $\mu\text{g/L}$. All reagents used were of at least analytical grade and all solutions were prepared with double-stilled water.

2.2 Experimental procedures

2.2.1 Microfluidic design

The microfluidic chip comprises 5 networks organized around a central outlet that serve as both cell injection hole and common waste reservoir (Fig. 1a). Each network comprises an up-stream gradient-generating module and a down-stream cell culture module. Channels stretched from cell chambers converge at the central outlet. The central outlet connected to a syringe pump, which is responsible for cell injection and fluids transport. Chemical reagents of different concentrations are loaded in two inlets of the gradient-generating module and driven to flow through the microfluidic networks. The branched microfluidic network serves to split, combine and mix fluid streams, generating six concentrations spanning two inlets at the terminals. Successive steps of diffusive mixing between adjacent laminar flow streams occur in the long channels to ensure complete mixing at the relevant flow rates. The microfluidic networks are symmetric, sizes of the horizontal part is 160 μm (width) \times 30 μm (depth), while that of the vertical part is 110 μm (width) \times 30 μm (depth). The total length of the serpentine channel is 53600 μm . At the end of the network, streams carrying different concentrations of the chemical reagent come into the adjacent cell culture chambers (2.5 mm \times 1.25 mm). A series of weir structures of arc shape were designed at the cell chambers to facilitate cell seeding through increasing contact area and slowing down flow speed. Regions of weir structure were defined as non-UV exposed areas thus were kept during the wet etching. The weir structures are of arch figure with a horizontal axis of 0.4 mm and a vertical axis of 0.12 mm. The width of the weir walls was 20 μm , and the horizontal and vertical distances between weirs were 0.2 mm and 0.45 mm, respectively.

2.2.2 Microfluidic device fabrication

The microfluidic chip is composed of a piece of glass plate and a covered PDMS film. Standard photolithography and wet etching method was used to fabricate the glass layer of the microfluidic chip [10]. Briefly, the schematic of microfluidic channels was drawn using the CAD software. The image was reproduced on a plastic film that serves as film mask for transferring microfluidic networks onto the glass plate by UV exposure. The photoresist was then developed to reveal the transferred image. Thus, all the area defining the channels was exposed. After serially rinsing with distilled water and acetone, the exposed area was etched with a diluted, stirred HF/ HNO_3 solution at 0°C to form channels. The etching rate in our experiment was about 1 $\mu\text{m}/\text{min}$. The etched plate was then bonded to a PDMS cover and kept at 80°C for 30 min. Holes of 3 mm diameter were drilled on the PDMS film at inlets and out-

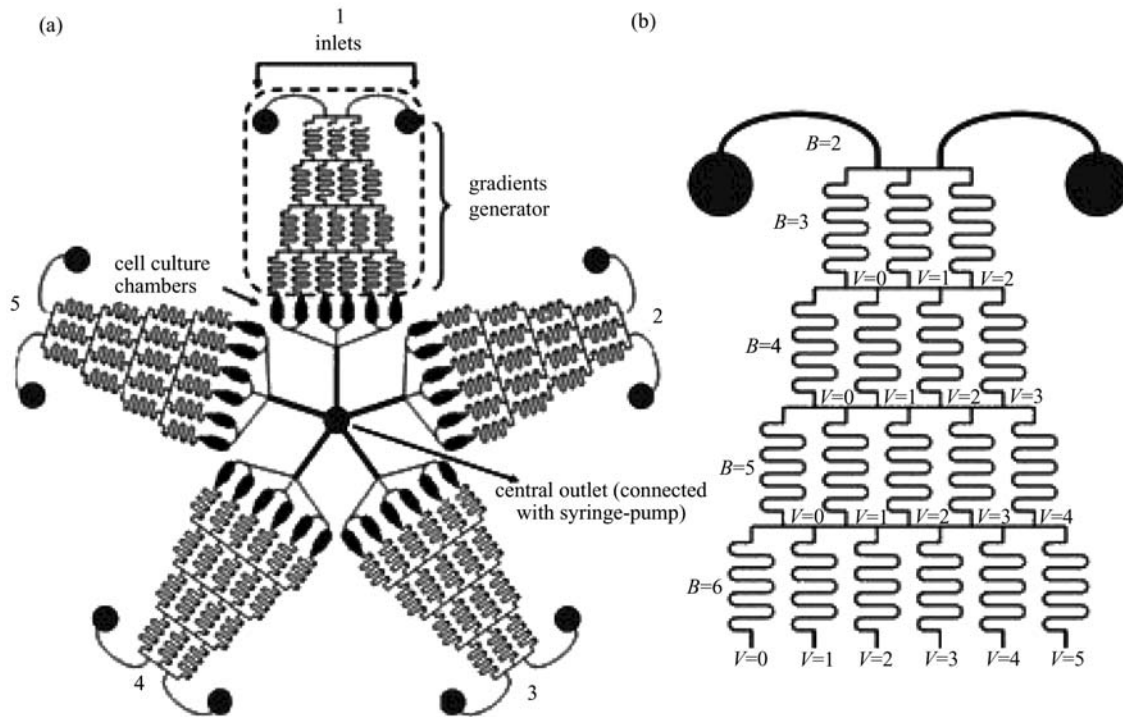


Fig. 1 (a) Layout of the microfluidic chip with 5 parallel gradient generators; (b) Schematic demonstration of the structure of the microfluidic network

lets. Plastic rings were affixed to the PDMS film with epoxy at inlet holes for cell culture medium loading. A circular silicone elastomer cover of 1 cm diameter and 6 mm height was sealed at the outlet, which was connected to a syringe pump through a Teflon tube.

2.2.3 Cell seeding, culture and stimulation on the microchip

Cells cultured in flask were harvested after treatment with 2.5% trypsin for 2 min at 37°C and centrifuge at 1000 r/min for 5 min. After the sediment was suspended in 500 μ L fresh medium, the number of cell in a drop of suspension was counted on a cell counting plate. Based on the count, the cell suspension was diluted to a concentration of 10^6 cell/mL. Cell suspension was injected to the microchip through the outlet at a flow rate of 0.2 μ L/s. Before fresh cell culture medium was added, cells were allowed to settle under static conditions for 6 h. Then, the cells were perfused with culture medium at a flow rate of 20 μ L/h overnight.

In each microfluidic network, cell culture medium containing chemical stimuli was added to one inlet, while blank medium was added to the other one. Cell culture medium containing 4 μ mol/L As_2O_3 was introduced to networks 1 and 2, while medium containing 5 mmol/L NAC was introduced to networks 3, 4, and network 5 with blank medium as a control group. The entire microfluidic device was moved to a cell culture incubator (37°C and 5%

CO_2), and then the fluid flow was driven by the syringe pump with negative pressure at a flow rate of 20 μ L/h. After 10 h stimulation, the chemical stimulation was removed. Networks 2 and 4 were further treated with culture medium containing 10 μ g/mL adriamycin for another 8 h, while the other networks were perfused with blank medium for the same period of time.

2.2.4 Cell staining and image analysis

The remaining cell culture medium was removed after stimulation and then fluorescent dye was added to both inlets. The intracellular GSH was labeled with NDA, which diffuses rapidly through the cell membrane and reacts with the intracellular thiol groups of GSH to form fluorescent products. An AO/EB morphological test was used to assess cell viability. AO is a vital dye that stains both live and dead cells, while EB stains only cells that have lost membrane integrity. Live cells will appear uniformly green, whereas necrotic cells will stain orange. Therefore, living cell rates can be calculated by the morphological assessment. High living rates indicate low chemotherapy sensitivity and vice versa. Cells treated with As_2O_3 (network 1) or NAC (network 3) were labeled with NDA to reflect the modulation of GSH level, and those further exposed to adriamycin (network 2 and 4) were labeled with AO/EB for viability tests. The cell array free of stimulation (network 5) were also labeled with AO/EB as a control group in which living cell rates higher than

95% are necessary. The cell chambers were serially treated with fluorescent dye for 15 min and cold PBS (4°C) for 5 min. After staining, cellular fluorescence was viewed on the fluorescent microscope.

Fluorescent images were analyzed using the WCIF ImageJ 1.37a software. The average fluorescence of each cell region was corrected for medium and device fluorescence as well as illumination fluctuations and non-uniformities by subtracting the average local background fluorescence. For NDA labeled cells, the result was scaled by the region area and divided by the number of cells in the region to determine average fluorescence density per cell in the region. For AO/EB labeled cells, cell viabilities were judged by the color of intracellular fluorescence.

3 Results and discussion

3.1 Laminar flow based concentration gradients generating microfluidic networks

The Reynolds number serves to measure the ratio of the inertial forces to the viscous forces. This ratio may be written as $Re = d\rho u/\mu$, where d , u , ρ , and μ are, the diameter of capillary, fluid speed, density and viscosity, respectively. On the basis of Reynolds number, flow patterns are usually classified into one of two kinds, turbulent and laminar flow. Laminar flow occurs at low Reynolds numbers ($Re < 2000$). The fluid dynamics are dominated by viscous drag rather than by inertia. In microfluidic channel with a width ranging from tens to hundreds of micrometers, the fluid flow that gives low Reynolds number has the characteristics of laminar flow. Therefore, the flow streams from different inlets run parallel to each other in the main channel. While flowing through microfluidic networks, the splitting, combining and mixing of flow streams generate a range of concentrations.

Figure 1(b) shows a photograph of a microfluidic network used for generating gradients. To calculate the concentration profiles at the outlets, it is necessary to know the relative ratios at which the streams are mixed together in the long serpentine channels. The mixing ratios are governed by the splitting ratios of the streams at the branching points in the network. To derive the equation for the splitting ratios, we define the part of the network that contains n vertical serpentine channels as a branched system of n th order, B (Branch) = n . Within each branched system of n th order, we label the vertical serpentine channels (V) from the left to the right, starting with $V = 0$ and ending with $V = m$, $m = B - 1$. The number of serpentine channels within a branched system increases by one going from a branched system of order n to a branched system of order $(n + 1)$.

In each microfluidic network, all serpentine channels have the same sizes and thereby have the same resistance

for the fluids. Since the fluidic resistance of the horizontal channels connecting the serpentine channels (width, 160 μm ; height, 30 μm ; length, 1 mm) is negligible in comparison with that of the long, serpentine channels (width, 110 μm , height, 30 μm , length, 13.5 mm), an equivalent circuit for the mathematical analysis can be approximated by taking into account the resistance of the serpentine channels only. Furthermore, the resistance of the serpentine channels is the same within each branched system. This fact forces the incoming streams in one branched system to distribute equally among the serpentine channels of the following branched system. As a result, the flux of fluid through each serpentine channel of a branched system is equal. The vertical mirror symmetry of the network demands that the splitting ratios are symmetric with respect to the axis of symmetry. By combining all of these boundary conditions, the following recursive formula governing the splitting ratios at the branching points are derived.

The portion of the stream that turns left is given by

$$(B - V_m)/B \quad (1)$$

The portion of the stream that turns right is given by

$$(V_m + 1)/B \quad (2)$$

As shown in Fig. 2, the two neighboring branched channels at lower levels accept streams from three channels at the upper level. Suppose concentrations of the incoming streams are C_d , C_e and C_f , and that of the combining streams are C_L (left) and C_R (right). According to Eqs. (1) and (2), the ratios of splitting in lower level channels were the left channel, $(V_d + 1)/B$ and $(B - V_e)/B$, right channel, $(V_e + 1)/B$ and $(B - V_f)/B$. The concentration of solution in lower level channels were:

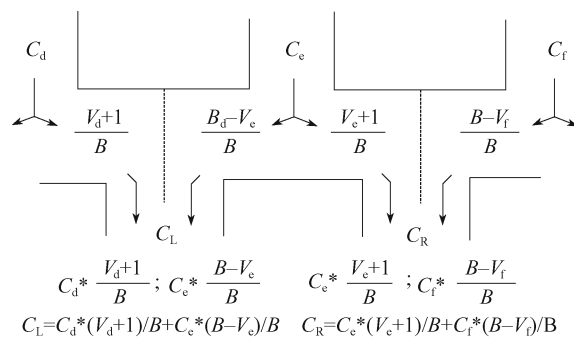


Fig. 2 Schematic demonstrating application of the formulas (1) and (2) calculating the splitting ratios at the branching points [6]

The dotted lines indicate the boundary between the two combined streams. The resulting concentrations can be calculated by the formula: in the left channel $C_L = C_d \times (V_d + 1)/B + C_e \times (B - V_e)/B$, while in the right channel $C_R = C_e \times (V_e + 1)/B + C_f \times (B - V_f)/B$.

$$C_L = C_d \times (V_d + 1) / B + C_e \times (B - V_e) / B \quad (3)$$

$$C_R = C_e \times (V_e + 1) / B + C_f \times (B - V_f) / B \quad (4)$$

In this work, every microfluidic network has two inlets. Suppose one inlet contains a solution of concentration C , the other contains blank solution of concentration 0. According to Eqs. (3) and (4), the concentration in a serials of six outlets at the terminals were: 0, $1/5 C$, $2/5 C$, $3/5 C$, $4/5 C$ and C . As the parallel networks have the same layout and size, the resistance of the networks is the same. With the same kind of fluid flowing in the networks, the income and flux of fluid through each network is equal.

3.2 Generation of parallel concentration gradients

Fluorescein sodium was used as an indicator to investigate the gradient pattern. In each network, $10 \mu\text{mol/L}$ fluorescein sodium was added to one inlet and PBS was added to the other one. The microfluidic networks were perfused at $20 \mu\text{L/h}$ for 12 h. The final concentration entering downstream cell chambers was monitored by fluorescence microscopy to quantify the stimulus and was found to remain steady throughout the experiment. The five dilution modules all generated concentration profiles of fluorescein sodium ranging from 0 to $10 \mu\text{mol/L}$ (Fig. 3). The result demonstrates that the laminar flow based parallel gradient generators provide precise control over the stability, gradient profile and concentration range of chemical gradient. The simultaneous gradient assay can be conducted easily by flowing two fluids in each network. The microfluidic device is able to generate parallel gradient concentrations to simulate the downstream cell arrays, by which morphological responses can be observed *in vitro* through a gradient concentration stimulation integrated assay. While these devices are robust and provide excellent control over the chemical gradient characteristics, they are suitable for addressing biological questions, including dose-dependent cellular response.

3.3 On-chip cell seeding and culture

After transfer to the chip chambers, the shape of MCF-7 cells changed from circular to multi-angular in 3 h, and to shuttle in 6 h. Through continuous observation, it was found that cells were evenly positioned in the chambers and adhere to the surface in 6 h (Fig. 4).

The suitability of the microchip for cell culture was determined using the AO/EB cell viability measurements. MCF-7 cells were seeded in the cell chambers and allowed to grow under flow conditions for 48 h prior to viability measurement. Cells are in good shape within 48 h on-chip culture. The AO/EB test shows that more than 95% viability over cells cultured in micro-chambers, and cell division was also routinely observed suggesting that the

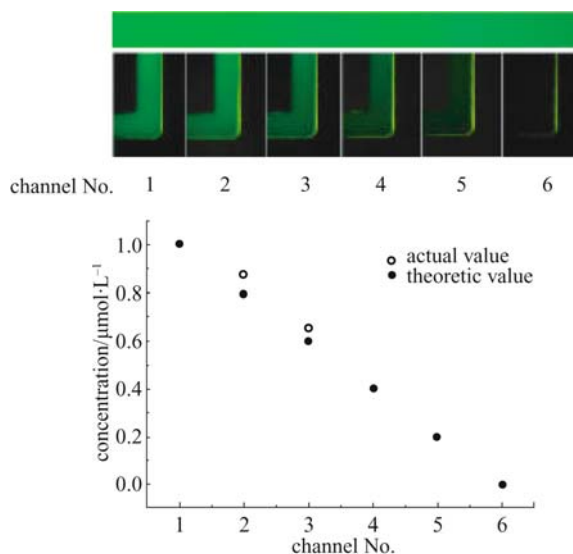


Fig. 3 Final fluorescein sodium concentration entering the downstream cell chambers in a microfluidic network, and the comparison of actual value and theoretic value of the concentration gradients profile (○ actual value, • theoretic value)

microfluidic device provided an environment conducive to cell growth and proliferation. Cell viabilities under conditions with chemical stimulation were also measured. After a 12 h treatment with As_2O_3 and NAC, cell viabilities are more than 90% in all chambers.

In our previous work using microchips without the weir structure design, cells cannot be evenly distributed. Being in close contact with each other, some cells hadn't enough space to spread properly for adhesion and were swept away in the following perfusion process. This problem was resolved by the design of a serial of weirs in the chambers, since these structures reduce disturbance to cell and increase contact area to the surface. Furthermore, chambers with weir structures provide a three dimensional space that suitable for cell growth.

3.4 Intracellular GSH levels upon chemical modulations

According to the theory of laminar flow based gradients generation, the dilute modules generate a series of linear concentration gradients spanning two inlets. Thus, the effect of chemical stimuli can be determined through dose dependent cellular responses. Upon As_2O_3 treatment, MCF-7 cells show decreasing intracellular GSH level with increasing As_2O_3 concentration; while upon NAC treatment, the intracellular GSH level increased with increasing NAC concentration (Fig. 5).

Arsenic is believed to exert some of its toxic effects through interaction with protein sulphhydryl groups and the non-protein sulphhydryl GSH [11,12]. Arsenite and GSH can react to form an $\text{As}(\text{SG})_3$ complex, which may contribute to the improved sensitivity to anticancer therapy by depletion of intracellular GSH. The GSH

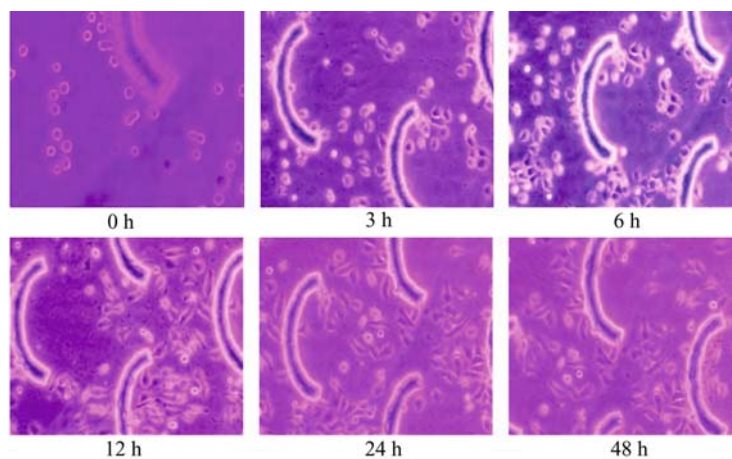


Fig. 4 Over time observation of MCF-7 cells cultured in the microchip for 48 h (20 ×)

Cells were in circle shape when transferred to the chamber, and showed change of shape in 3 h, properly stretched in 6 h. In a continuous observation, cells were found morphologically healthy within 48 h.

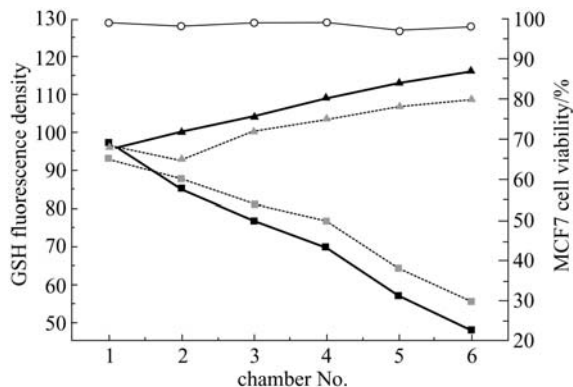


Fig. 5 Intracellular GSH level and cell viabilities upon treatment with gradient concentration of As₂O₃ and NAC (■ GSH fluorescence with As₂O₃ treatment; □ cell viability with As₂O₃ treatment; ▲ GSH fluorescence with NAC treatment; △ cell viability with NAC treatment; ○ cell viability in control chambers)

precursor NAC was converted intracellular to the rate limiting substrate for GSH synthesis, by which GSH concentrations was augmented [13].

3.5 Relationship between chemotherapy sensitivity and intracellular GSH level

GSH is the most abundant intracellular thiol, serving as a critical cellular antioxidant. The reduction-oxidation (redox) status of a cell is largely determined by the balance between reactive oxygen species (ROS) generated and endogenous expression of thiol buffers such as GSH [14]. As the preferred substrates of multi-drug resistance related protein1 (MRP1) transporter are GSH-conjugates, GSH can similarly detoxify many exogenous toxins with positive charge, including chemotherapeutic drug, through the formation of GSH adducts. Several studies suggest that GSH is involved in resistance to

cytotoxic drugs through the formation of GSH adducts [15–17].

In this work, the chemotherapy sensitivity of MCF-7 cells shows a dose-dependent relationships with cellular GSH level that are modulated by the on-chip gradient concentration chemical stimulation. As shown in Fig. 5, chemotherapy sensitivity is correlated to intracellular GSH level. Suppression of intracellular GSH by treatment with As₂O₃ has been shown to increase chemotherapy sensitivity. Conversely, elevation of GSH production by treatment with NAC leads to increased drug resistance. These results indicate that total cellular GSH content is an important determinant of chemotherapeutic drug resistance. One explanation for arsenic induced drug resistant reversal is the inhibition of the activity of GSH S-transferase [18], in which the decreased activity of GSH S-transferase has been associated with incapacity to catalyze the coupling of GSH to multiple reactive substrates. The results of this work indicate that besides the activity of GSH S-transferase, total cellular GSH content is also an important determinant of chemotherapeutic drug resistance.

4 Conclusion

A microfluidic chip featuring parallel gradient generating networks was developed and applied for the study of drug resistance of MCF-7 cells. The results show that the microchip was suitable for cell culture and gradient concentration chemical stimulation. Intracellular GSH level and drug sensitivity of MCF-7 cells show dose-dependent relationships with concentrations of chemical stimulus. The microfluidic chip offers an opportunity to integrate the whole procedure of cell-based pharmacological profiling, including cell seeding, cell culture, concentration gradients generation, drug stimulation, molecule labeling and cellular responses monitoring. The microchip based assay

enables multifactor and multiparametric analysis, thus holding great potential for extrapolation to high-content drug screening.

References

1. El Ali J, Sorger P K, Jensen K F. Cells on chips. *Nature*, 2006, 442(7101): 403–411
2. Chen X, Cui D F, Liu C C, Cai H Y. Chinese J Anal Chem, Microfluidic biochip for blood cell lysis, 2006 34(11): 1656–1660 (in Chinese)
3. Wu J G, Yue R F, Zeng X F, Kang M, Hu H, Wang Z Y, Liu L T. Studies on digital microfluidic chip for Micro-Total-Analysis systems. Chinese J Anal Chem, 2006, 34(7): 1042–1046 (in Chinese)
4. Weigl B H, Bardell R L, Cabrera C R. Lab-on-a-chip for drug development. *Adv Drug Deliv Rev*, 2003, 55(3): 349–377
5. Jeon N L, Dertinger S K, Chiu D T, Choi I S, Stroock A D, Whitesides G M. Generation of solution and surface gradients using microfluidic systems. *Langmuir*, 2000, 16(22): 8311–8316
6. Dertinger S K, Chiu D T, Jeon N L, Whitesides G M. Generation of gradients having complex shapes using microfluidic networks. *Anal. Chem*, 2001, 73(6): 1240–1246
7. Jeon N L, Baskaran H, Dertinger S K, Whitesides G M, van de Water L, Toner M. Neutrophil chemotaxis in linear and complex gradients of interleukin-8 formed in a microfabricated device. *Nat Biotechnol*, 2002, 20(8): 826–830
8. Saadi W, Wang S J, Lin F, Jeon N L. Biomed. A parallel-gradient microfluidic chamber for quantitative analysis of breast cancer cell chemotaxis. *Microdevices*, 2006, 8(2): 109–118
9. Thompson D M, King K R, Wieder K J, Toner M, Yarmush M L, Jayaraman A. Dynamic gene expression profiling using a microfabricated living cell array. *Anal Chem*, 2004, 76(14): 4098–4103
10. Liu D Y, Shi M, Huang H, Long Z, Zhou X, Qin J, Lin B C. Isotachopheresis preconcentration integrated microfluidic chip for highly sensitive genotyping of the hepatitis B virus. *J. Chromatogr B*, 2006, 21(844): 32–38
11. Vahter M, Concha G. Pharmacol. Role of metabolism in arsenic toxicity. *Toxicol*, 2001, 89(1): 1–5
12. Shimizu M, Hochadel J F, Fulmer B A, Waalkes M P. Effect of glutathione depletion and metallothionein gene expression on arsenic-induced cytotoxicity and c-myc expression *in vitro*. *Toxicol Sci*, 1998, 45(2): 204–211
13. Yim C Y, Hibbs J B, Mcgregor J R, Galinsky R E, Samlowski W E. Use of N-acetyl cysteine to increase intracellular glutathione during the induction of antitumor responses by IL-2. *J Immunology*, 1994, 152(12): 5796–5805
14. Davis W J, Ronai Z, Tew K D. Cellular thiols and reactive oxygen species in drug-induced apoptosis. *J Pharmacol Exp Ther*, 2001, 296(1): 1–6
15. Schroder C P, Godwin A K, O'Dwyer P J, Tew K D, Hamilton T C, Ozols R F. Glutathione and drug resistance. *Cancer Invest*, 1996, 14(2): 158–168
16. Anderson M E. Glutathione: an overview of biosynthesis and modulation. *Chem Biol Interact*, 1998, 111/112: 1–14
17. Ishikawa T, Ali Osman F. Glutathione-associated cis-diamminedichloroplatinum(II) metabolism and ATP-dependent efflux from leukemia cells. Molecular characterization of glutathione-platinum complex and its biological significance. *J Biol Chem*, 1993, 268(27): 20116–20125
18. Shiga H, Heath E I, Rasmussen A A, Trock B, Johnston P G, Forastiere A A, Langmacher M, Baylor A, Lee M, Cullen K. J. Prognostic value of p53, glutathione S-transferase pi, and thymidylate synthase for neoadjuvant cisplatin-based chemotherapy in head and neck cancer. *Clin Cancer Res*, 1999, 5(12): 4097–4104